Journal of the Korean Physical Society, Vol. 43, No. 4, October 2003, pp. 607∼615

Recent Topics in Engineering for Solid-State Peak-Power Lasers in Repetitive Operation

Masahiro NAKATSUKA,* Hidetsugu YOSHIDA, Yasushi FUJIMOTO, Kana FUJIOKA and Hisanori FUJITA
Institute of Laser Engineering, Osaka University Suita, Osaka 565-0781, Japan

(Received 7 July 2003)

Solid-state lasers have been developed for peak-power operation in the terawatt to petawatt regions by using chirped pulse amplification (CPA) and optical parametric (OPCPA) technology. Also thermal distortion-free, 10-nsec repetitive peak-power lasers have been developed. Broadband amplification of a solid-state laser is a key issue for the pre-amplification stage of CPA system, and the OPA scheme gives a high gain with a very low pre-pulse level while keeping a 5-nm bandwidth. On the other hand, nonlinear optical technology using stimulated Brillouin scattering (SBS) is promising as a way to compensate for thermal difficulties caused in strongly pumped laser materials. SBS is well known for the phase conjugation mirror (PCM) used for an average power output with a high reflectivity of over 95 %. A liquid fluorocarbon with a special treatment can be used to achieve a 10-ns duration, 50-Hz repetition laser delivering 0.4-GW peak power, with a 200-W average power. A liquid flow system in an SBS cell can be used to realize PCM behavior up to the kW range. The last theme in this paper is a short review of new ceramic materials for a scalable solid-state laser. In past ten years, Japanese researchers have investigated new transparent ceramic YAG materials for industrial application. The ceramics have many advantages for an average power laser, such as high doping rate, co-doping potential, large-size fabrication, and composite structure.

PACS numbers: 42.60.By, 42.55.Rz
Keywords: Solid-state lasers, Peak-power lasers, Chirped pulse amplification, Optical parametric technology, New ceramic YAG materials

I. INTRODUCTION

Recently, solid-state laser terawatt to petawatt peak power laser with CPA (chirped pulse amplification) and OP (optical parametric) CPA have been developed to operate in the sub-psec region. Also, thermal distortion-free tens of nsec peak-power YAG lasers with repetitive high-average output have been developed. For the inertial fusion research at the Institute of Laser Engineering, Osaka University, a fast ignition scheme was adopted to achieve a hot core-plasma at keV-temperature by heating additionally a dense plasma imploded by using ofmulti-beam laser system. Figure 1 shows the history of development of sub-ps laser systems, including dye, Nd:glass and Ti:sapphire lasers.

The glass laser is now the most powerful one for a one-shot base design. Broadband amplification is a key issue for the amplification stage of a CPA system. Optical parametric amplification (OPA) gives high gain with very low pre-pulse generation while maintaining a bandwidth of several nm. In this report, the OPA technique is described in the next section. On the other hand, the average operating power of solid-state lasers is strongly affected by the thermal problems in the laser materials. The nonlinear optic technology of stimulated scattering is a promising one for compensating for thermal problems caused in strongly pumped laser materials. Stimulated Brillouin scattering (SBS) is well known for phase conjugation mirrors (PCM) to be used in average power outputs with high reflectivity over 95 %. A liquid fluorocarbon with special treatment produces a 10-ns, 50-Hz

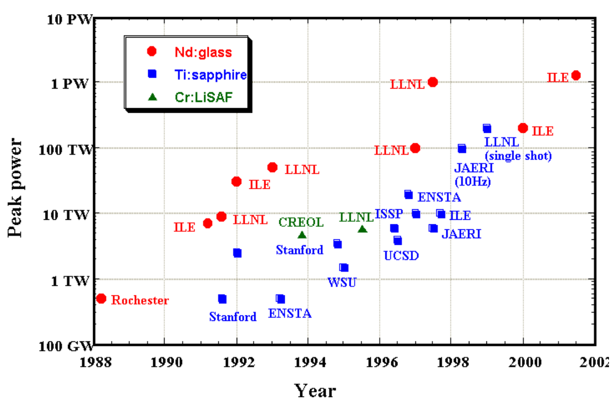

Fig. 1. Historical development of sub-ps laser systems. Abbreviation shows many famous institutes of the world.

*E-mail: naka@ile.osaka-u.ac.jp; Fax; +81-6-6877-4799

repetitive pulse delivering a peak power of 0.4 GW peak and an average power of 200 W. The liquid flow system helps the PCM behavior up to the kW range. In the third section, PCM technology developed in Japan is reviewed. The total output energy of peak-power lasers is limited, of course, by the volume and the diameter of the laser materials. YAG is an excellent host crystal, but its scale is limited by the fabrication process.

Lastly described here is a short review of new ceramic materials for a scalable solid-state laser. During the past ten years, Japanese researchers have been investigating a new transparent ceramic YAG material for industrial applications. The ceramic medium has many advantages for average power laser, such as a high doping rate, co-doping potential, large-sized fabrication, and a composite structure. Various features of ceramic materials are discussed in Section IV.

II. OPCPA TECHNOLOGY FOR SHORT-PULSE AMPLIFICATION

1. PW System for Fast Ignition

The fast igniter study requires intense chirped pulse amplification (CPA) in large-scale Nd:glass laser systems at a 1.053-μm wavelength. The front-end of a petawatt laser consists of ultra-short pulse pre-amplifiers with OPCPA technology, a booster amplifier chain with a 350-mm aperture glass laser, and a large aperture-grating compressor. This system enables us to achieve 1 PW within a pulse duration of several hundreds of femtoseconds and with a focused intensity $> 10^{20}$ W/cm^2 in a 40-μm focal spot. We developed a petawatt module laser system (abbreviated as PWM) in 1997, which has been upgraded to the petawatt (PW) laser now. The front-end system has a broadband high-gain OPCPA to generate appropriate chirped pulses.

The front-end for the PW Nd:glass laser currently uses a Ti:Al_2O_3 regenerative amplifier that possesses a broadband spectrum ($0.6 \sim 1.1$ μm). However, the single-pass gain is very low at a 1-μm wavelength because the cross-section is about one-tenth that at 0.8 μm. As a result, the regenerative amplifier needs from 70 to 120 round trips to achieve a sufficient gain of over 10^6 at a 1-μm wavelength. The output bandwidth is limited to the spectral transmittance of the cavity components, such as the polarizer and the Pockels cell. The pulse contrast ratio is as low as $10^{-3} \sim 10^{-4}$ due to high-level ASE (amplified spontaneous emission) and pre-pulses.

OPCPA [1–3] has the potential for high-energy ultrafast pulse amplification. The advantages of the OPCPA technique are (1) high gain in single-pass amplification, (2) high beam quality due to low heat deposition, (3) a small B-integral, (4) a high contrast ratio, and (5) an extremely broad gain bandwidth. With an OPCPA system using a large-sized KDP crystal, it will be possible to obtain a multi-PW output. We present an experimental study of a high-gain OPCPA system. The OPCPA is much more compact, and its gain is higher than the currently used regenerative amplifier or multi-pass amplifier at 1-μm wavelength, thus ensuring stable operation.

2. New Front-end Laser System

The new front-end consists of a passively mode-locked diode-pumped Nd:glass laser, a first pulse stretcher, an OPCPA-I as a pre-amplifier, a second pulse stretcher, and an OPCPA-II as a main-amplifier. The front-end system was newly set in the GEKKO XII oscillator room and delivered, with precise timing, a seed pulse for the GEKKO system.

The diode-pumped laser has a semi-conductor saturable absorber mirror (SESAM) to generate a 150-fs pulse train of 100 mW at a tunable center wavelength of $1.051 \sim 1.061$ μm. The full width at half maximum (FWHM) spectral width is 8.5 nm around 1.054 μm. The output pulses are synchronized to the RF signal (99.998 MHz) within a few ps by controlling the cavity length by using a PZT actuator. A single pulse from the pulse train is selected by the Pockels cell (contrast ratio, 10^{-3}) and is temporally stretched from 150 fs to 1.5 ns by the first stretcher, which is a 3.2-m long and is formed by a 1485-lines/mm diffraction grating pair coupled by a confocal telescope. The gratings are set at a 47° incident angle designed for a chirping rate of 250 ps/nm. The 6-nm bandwidth and the 1.5-ns stretched pulse width are obtained by spectral clipping due to the clear apertures of the lenses and the gratings. The output pulse is injected into the preamplifier OPCPA-I.

The output pulse of OPCPA-I is again stretched from 1.5 ns to 3 ns by the second stretcher. A combination of a high reflectance mirror and a telescope lens in a double-pass configuration can change the length of the stretcher in a precision of $\pm$10 cm for a correct stretching. The stretched pulse is seeded into the OPCPA-II system. A monitor measures the pulse width by using small compressor optics. The PW laser is synchronized to the GEKKO XII laser with a timing jitter within 10 ps. Table 1 lists the design parameters of the front-end system.

3. Experimental Results of OPCPA

The pulse energy seeded to OPCPA-I is about 0.4 nJ at a 1.5-ns pulse duration. The overall transmitted efficiency from the oscillator is 40 %. The OPCPA amplifier is operated with two amplification stages of β-barium borate (BBO) crystals. Figure 2 shows the optical layout of OPCPA-II. The BBOs are cut at 22.8° for type-I angular phase matching. The optically pumping light

Table 1. Design parameters of a front-end system.

Spectral width	> 6 nm (oscillator; 8 nm)
Pulse width	> 3 ns (oscillator; 150 fs)
Central wavelength	1053 ∼ 1055 nm
Contrast ratio to pre-pulse	$>10^8$
Output energy	>10 mJ
Output beam diameter	3 ∼ 5 mm
Energy stability	95 %
Pointing stability	<100 μrad

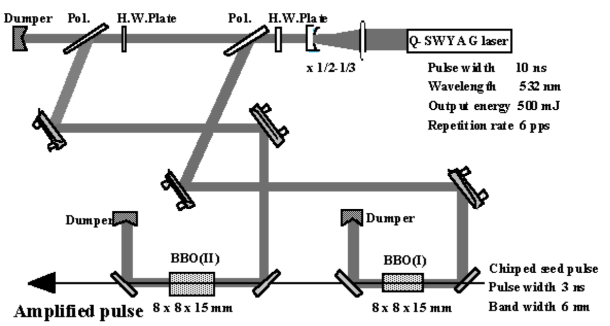

Fig. 2. Optical layout of OPCPA-II.

Table 2. Pumping parameters of two OPCPA systems.

	OPCPA-I	OPCPA-II
BBO crystal size	5 × 5 × 15 mm	8 × 8 × 15 mm
	+ 5 × 5 × 18 mm	+ 8 × 8 × 15 mm
Pump pulse width	6 ns	10 ns
Seed pulse width	1.5 ns	3 ns
Total pump energy	150 ∼ 200 mJ	400 ∼ 500 mJ
Pump peak intensity	700 MW/cm^2	550 MW/cm^2

is the frequency-doubled output (0.532 μm) of a single-transverse-mode Q-switched Nd:YAG laser operated at a repetition rate of 6 Hz. The single-transverse-mode laser is used to ensure a smooth temporal profile to prevent spectral modulation of an amplified chirped pulse. The output of pump beam is separated into two stages of the amplifier by using a combination of a half-wave plate and a thin film polarizer. The pump-beam diameter on the crystals of OPCPA-I and -II are about 2 mm and 5 mm, respectively. The maximum pump energy of OPCPA-I and -II are about 200 mJ and 500 mJ, respectively. The seed beams are horizontally polarized and the pump beams are vertically polarized. The pumping parameters of the two OPCPA systems are shown in Table 2.

In OPCPA-I, the gain of the first stage is 10^3. When the pump intensity of the second stage is 700 MW/cm^2, the maximum total gain is 1.5 × 10^6. The maximum output energy is about 0.6 mJ. The spectral bandwidth of the amplified pulse is almost same as that of the seed

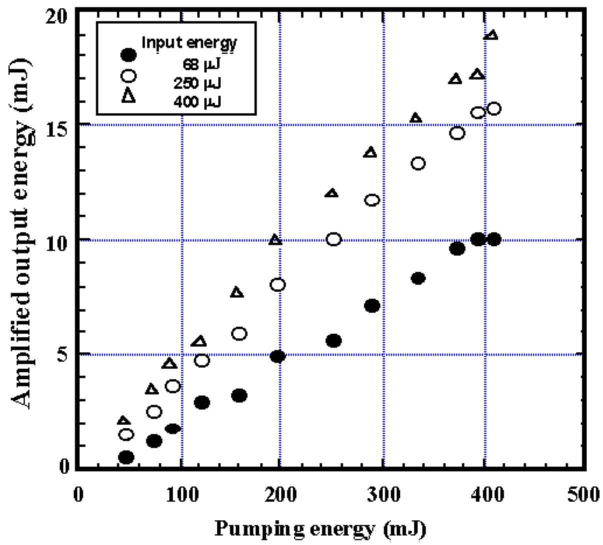

Fig. 3. Amplified output energy as a function of the pumping energy.

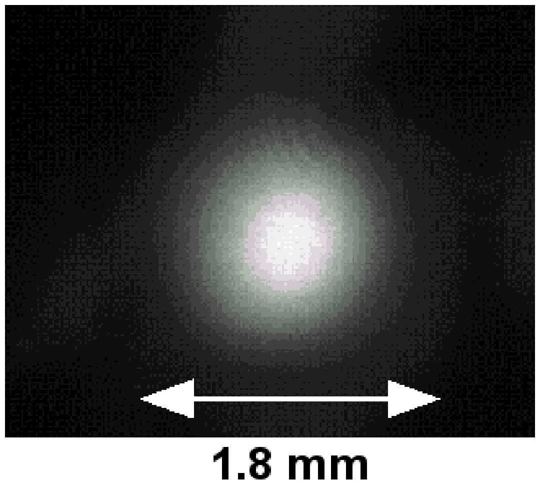

Fig. 4. Near-field pattern.

pulse (6-nm bandwidth) [4]. In OPCPA-II, the small signal gain of the two-stage power amplifier is >700 at a peak pumping intensity of 550 MW/cm^2. The saturated gain is around 50 with a conversion efficiency of 4.8 % at a seeding energy of 0.4 mJ. Figure 3 shows the output energy as a function of the pumping energy [5].

The measured spectral width of the amplified pulse is apparently enlarged in the saturation region. The maximum spectral width was measured to be 8 nm, which was 30 % broader than the incident spectrum. It should be noted that temporal broadening in the OPCPA causes spectral broadening. The output beam profile had a very smooth Gaussian shape with a FWHM diameter of 1.8 mm as shown in Fig. 4. An output energy fluctuation of ±8 % has been demonstrated under a gain-saturated condition and can be minimized by further improvement of both the energy stability and the timing jitter of the pump pulse.

We have constructed a front-end system using a broad-band high-gain OPCPA for chirped pulse amplification. This system can deliver output energy of 20 mJ with a 6-nm spectral width at a center wavelength of 1.053 μm. These output parameters are appropriate as a seed for a high-peak-power Nd:glass laser system.

III. SBS-PCM FOR REPETITIVE PEAK-POWER LASER

1. Phase Conjugation for a Repetitive Laser

In this report, topical technology for phase compensation of a conventional highly pumped rod YAG laser is introduced. An improvement in the output energy of a multi-stage YAG laser system was achieved by using a stimulated Brillouin scattering (SBS) phase conjugation mirror (PCM). The phase conjugation of the optically nonlinear SBS process in a liquid material compensated perfectly for thermal degradation due to the repetitive peak-power amplifier, resulting in an average power increase from 1 $\sim$ 2 J at a 30-Hz repetition to 3 $\sim$ 5 J at a 50-Hz drive. The beam quality was also recovered without a wavefront deformation and depolarization and had a diffraction-limited divergence with a goodflattop pattern in the near field.

The stimulated Brillouin scattering-phase conjugation mirror (SBS-PCM) is an important tool for improving the performance of high-power laser systems [6]. Phase conjugation can improve the image quality due to compensation of thermally induced wavefront distortion in the medium or to some poor components. SBS elements in compact high-peak-power laser systems have been reported previously [7–11] and application of SBS to large facilities, such as inertial confinement fusion (ICF) systems, has been proposed [12]. Efficient and safe SBS media are necessary for further development of high-power laser systems. A possible approach is in the selection of a medium to support SBS.

For the plasma diagnostics of Thomson scattering by using a Nd:YAG solid-state laser, a high peak power, a high repetition rate, and good beam quality for tight focus in a stable operation are required. The YAG laser usually used consists of a MOPA (master oscillator and power amplifier) system, and at JT-60U, JAERI, Japan, it was designed to deliver 1.0 $\sim$ 1.5 J at a 30-ns pulse width in a 30-Hz repetition, and average power of 30 $\sim$ 40 W. The original near-field pattern (NFP) of output beam before using the SBS cell is shown in top of Fig. 7.

A peak power laser with several-nanoseconds duration is very suitable for use as an SBS-PCM for the medium threshold energy and average power. In recent years, in order to achieve high- performance SBS mirrors, several materials in liquid or solid phases with very high laser-damage thresholds were discovered [13]. We demonstrated that a closed-type single-cell SBS-PCM enables the incident power to reach the 100-W level, thus, a drastic improvement of the laser performance was achieved [14].

The YAG laser/amplifier system used in the Thomson scattering at JT-60U is a conventional MOPA system that uses a linearly polarized, multi-transverse mode, TEMoo Q-switched oscillator delivering a 30-mJ, 20-ns quasi-Gaussian waveform pulse. The output is amplified by two 10 mm$^{\phi}$ $\times$ 100mm^{l} Nd:YAG-rod preamplifiers. The main amplifier consists of two 8 mm$^{\phi}$ $\times$ 100 mm ^{l} Nd:YAG amplifiers and two 14 mm$^{\phi}$ $\times$ 100 mm^{l} amplifiers. The final output is 1 J in pulse duration of 20 ns, with a divergence of <0.5 mrad (half angle) at a 30-Hz repetition rate [15]. As the pumping power was increased, the NFP becomes poor in shape as the result of the thermally induced lens effect, the birefringence effect, and the diffraction by the rod edge. The measured depolarization loss in a single pass through the two YAG rods (14-mm diameter) is only about 3 to 5 % with birefringence compensation using a 90-degree rotator.

2. SBS Materials and PCM Reflectivity

We have used Fluorinert FC-75 as an SBS medium. Liquid fluorocarbons satisfy the demands for an SBS medium owing to their excellent optical quality, low absorption in a wide spectral region from the ultraviolet to the infrared, high optical breakdown threshold, good thermodynamic property, and highly desirable chemical stability. Heavy perfluorocarbons are stable liquids at room temperature and atmospheric pressure. Mixtures of heavy perfluorocarbons are available as Fluorinert (FC), manufactured by 3M-Company, U.S. The C-F bonding energy of 5.56 eV and the high ionization potential are responsible for their high dielectric breakdown strength.

SBS reflection for single shot operation starts from a 3-mJ threshold, and the reflectivity reaches 98 % at a 1.4-J input with TEMoo single frequency pumping, which is 3000 times its threshold, without breakdown as shown in Fig. 5.

3. Improvement of Laser Performance

Figure 6 shows the YAG laser/amplifier system with SBS-PCM at a 30- to 50-Hz repetition rate. An SBS-PCM is installed in each of the multi-stage YAG amplifiers to change the amplification arrangement from a single pass to a double pass. A 90-degree rotator is inserted between amplifiers to compensate for the depolarization induced in the laser rod by passing a beam through an orthogonally- rotated position in a rod each other. Image-relay telescopes are used to minimize the

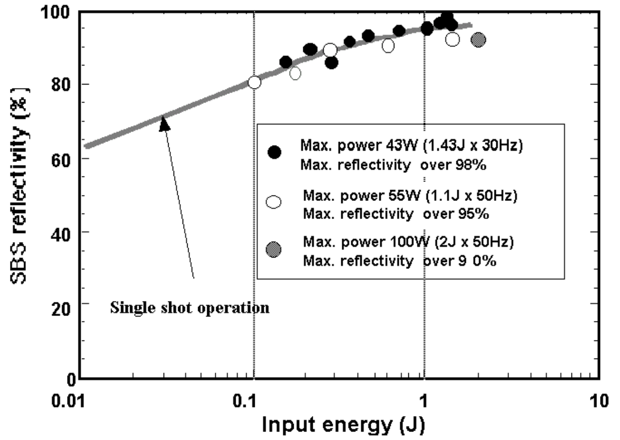

Fig. 5. SBS reflectivity of a single-mode pump beam as a function of the input energy focused onto a SBS cell at a repetition of 30 Hz.

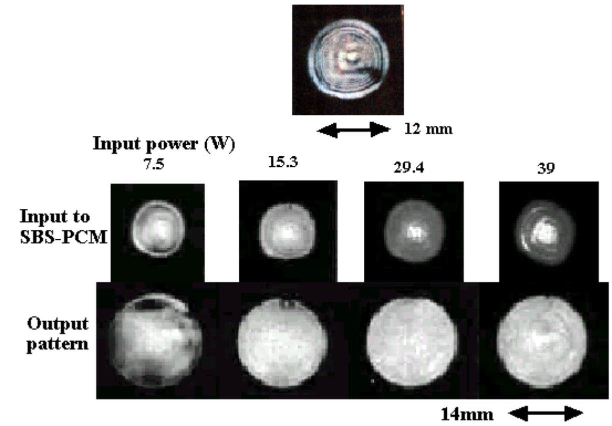

Fig. 7. Output beam pattern without PCM (upper) and with SBS-PCM (lower).

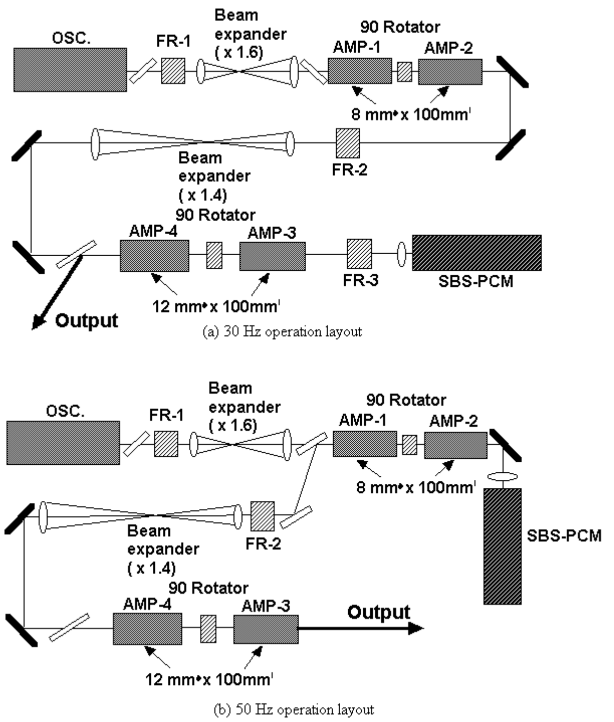

Fig. 6. YAG laser amplifier system with SBS-PCMs for the Thomson scattering light source at JT-60U.

effect of diffraction and to maintain beam uniformity. The beam image of the oscillator output beam is image-relayed into an amplifier head. A thin film polarizer realizes output coupling, and a 90-degree rotation is carried out by a Faraday rotator that is passed twice. The amplified output beam is focused at a point of 150-mm inside a 300-mm long SBS cell by a lens with a focal length of 200 mm. The SBS reflectivity measured in Fig. 5 is defined as the ratio between the energy reflected from the SBS mirror and the energy incident on the cell. The maximum input power to the SBS cell is 100 W at 50 Hz. A reflectivity of approximately 98 % is obtained at an incident energy of 1.43 J. The transmitted power is only 1.4 W at a 53-W input power, and about 10 W at a 100-W input. The SBS reflectivity in a repetitively rated operation is similar to that of the single-shot operation. No optical damage was observed during the experiment. As the incident energy is increased, the SBS reflectivity increases slowly, and the reflection point in the cell moves towards the cell entrance. As a result, optical breakdown does not happen because the focused intensity does not increase too much.

The most interesting parameter of the SBS-PCM is the fidelity of the reflected beam. The NFPs of the input, the amplified output and the transmitted beams through the SBS-PCM are shown in Fig. 7. The thermal effect in the laser rod by due to strong pumping, such as thermal lensing and depolarization, suppresses the average power level because of the off-axis ray trajectory with aberration and polarizing loss. A good flattop pattern was achieved due to the diffraction fringes being reduced as a result of the spatial filtering by SBS. The modal reflectivity follows the intensity at the beam waist so that higher-order spatial frequencies feel a weak reflectance. The SBS-PCM works as a low-pass filter even without a soft aperture.

The spot size of the reflected beam was recorded in the far field pattern (FFP) diagnostic as a function of the input energy. The focal spot size of the reflected beam was only 1.5 times the diffraction-limited size. Shot-to-shot intensity fluctuations were not observed in the FFP.

This system successfully demonstrated a maximum output power of 130 W and a peak power of 170 MW. The maximum pulse energy reached 2.6J for a 15-ns pulse width at a repetition rate of 50 Hz. The incident and the reflected pulses showed almost the same shapes with the exception of the leading edges.

The undesirable effect competing with SBS is the local thermal deformation of a beam due to self-defocusing caused by laser-beam absorption in the gaseous and the liquid materials. Localized heating in the interaction region, especially near the focal point, might deleteriously influence generation of the SBS phase conjugation wave. The transient critical energy, E_{cr}, which corresponds to the energy at the beam waist and reduces to one half an original energy density due to a thermal diffusion of laser light for a single-shot operation, can be written as follows [16]:

$$E_{cr} = \frac{2\pi \cdot \rho \cdot C}{\left|\frac{dn}{dT}\right| \cdot \alpha \cdot \left(\frac{2\pi}{\lambda}\right)^2}, \qquad (1)$$

where λ, n, $\rho \cdot C$, T, and α are the pumping wavelength, the refractive index, the medium density, the specific heat, the temperature, and the absorption coefficient, respectively. For SBS generation, the incident energy E_{in} must exceed the SBS threshold energy E_{th}. Therefore, the energy transmitted through the focal waist must be more than E_{th}. The product, f^*E_{tr}, of the repetition rate f and the transmitted energy E_{tr} for a single shot may not exceed the critical energy E_{cr}. The critical energy E_{cr} of Fluorinert FC-75 is calculated to be about 5 J from the absorption coefficient of 3×10^{-6} cm^{-1}. This critical energy is the highest known for SBS liquids because the absorption coefficient is very low over a wide spectral range (0.2 $\sim$ 4 μm). The total transmitted energy in this experiment was about 2.75 J, which was 5 % of the total incident energy of 55 J. This value is much lower than the calculated critical power. If the SBS reflectivity is over 90 %, an incident energy of 50 J can be injected into the SBS-PCM.

The critical pulse duration, t_{cr}, above which thermal self-defocusing occurs when a threshold, P_{th}, equal to the SBS threshold goes to the focus waist can be written as $t_{cr} = E_{cr}/P_{th} = E_{cr}/(E_{th}/t_L)$, where t_L is the pulse width. The critical pulse duration tcr for a repetitive pulse laser must be greater than the thermal diffusion time $t_d = S/D$, which depends on the crosssection of the focal waist S and a thermal diffusivity D. The thermal diffusion coefficient is 3.7×10^{-4} cm^2/s for Fluorinert FC-75. As convection due to the temperature distribution occurs in absorbent liquids, a refractive-index change in the SBS cell scatters a fraction to the defocused beam. The thermally induced rate of change in the refractive index, dn/dT, is -4.2×10^{-4} K^{-1} for Fluorinert FC-75. The diffusion time t_d is less than $t_{cr}/(t_L f)$ for repetitively pulsed lasers. For example, when a transverse-mode diffraction-limited beam is focused with F = 200 mm, $S = 1.4 \times 10^{-5}$ cm^2, and D = 3.7×10^{-4} cm^2/s, the thermal diffusion time t_d is 3.7×10^{-3} s. When the operation condition is f = 50 Hz, t_L = 30 ns, and $t_{cr} = 5 \times 10^{-5}$ s, the condition of $t_d < t_{cr}/(t_L f)$ is satisfied.

4. Future of YAG Lasers

Table 3 shows the laser performance of several optical layouts tested for a Nd:YAG laser system. An average output power of 250 W is produced at a 50-Hz repetition rate by two lines of YAG amplifiers, one with a 12-mm diameter YAG rod and the other with a 14-mm rod with the SBS-PCM. We have prepared a new flow-type cell and a wedge-plate rotation method [17,18] that enables to remove the thermally induced defocusing and convection due to laser light absorption in the SBS cell.

An improvement in the output beam power/quality of a multi-stage YAG laser system with an SBS-PCM was achieved. The phase conjugation of the optically nonlinear SBS process in a liquid material compensated perfectly for the thermal degradation due to the average/peak power amplifier, resulting in an average power increase from 1.5 J at a 30-Hz repetition to 2.6 J at a 50-Hz drive. A high peak power laser, such as a few J with a few kHz repetition rate, based on SBS-PCM is very suitable as a laser source for extreme ultraviolet (EUV) light generation for semiconductor lithography.

IV. NEW CERAMIC YAG MATERIALS

Scientific and industrial applications need more energy and a higher peak power from lasers that are limited in design and performance by the size of the lasing material and the staging of the system. YAG is the best crystal for a laser host. However, conventional crystal-growing methods produce crystals that are only 2 cm in diameter and 20 cm in length, and the doping rate with rare-earth ions is limited to around 1 %.

1. Recent Development of Ceramic Materials

In the last ten years, Japanese researchers invented and developed new fabrication methods for perfectly transparent YAG ceramics for use as a laser host [19–21]. Polycrystalline ceramic YAG shows the same characteristics, such as the emission cross-section, thermal constants, mechanical property, and so on, as a single crystal. In addition, the range of doping with lasing ions was expanded to over 10 % from 1 %.

The technology to grow a polycrystalline (ceramic) material includes the following processes: production of a YAG precursor from a chemical composition or a sol-gel in liquid phase, calcinations to fine YAG particles, casting of fine powder to a final shape by slurry processing, and finally sintering of a molded YAG to a transparent ceramic. The scalability of ceramics was verified fabricating a 20 $\sim$ 30 cm laser slab [22]. The size of the final product depends only on the scale of the sintering furnace.

Developing ceramics technology will enhance the possibility of using a wider variety of laser ions, which are

Table 3. Laser performance with and without SBS-PC. "2p" means two heads of amplifier in the serial arrangement.

Optical layout	Pulse energy (J)	Rep. rate (Hz)	Power (W)
(1) MOPA (8-mm rod × 2p) + (12-mm rod × 2p without SBS-PCM)	1.5	30	45
(2) (8-mm rod × 2p) + (14-mm rod × 2p with SBS-PCM)	2.1	30	62
(3) (8-mm rod × 2p with SBS-PCM) + (14-mm rod × 2p)	2.6	50	130
(4) (8-mm rod × 2p) + (14-mm rod + 12-mm rod with SBS-PCM in two lines)	5 ∼ 6	50	250 ∼ 300

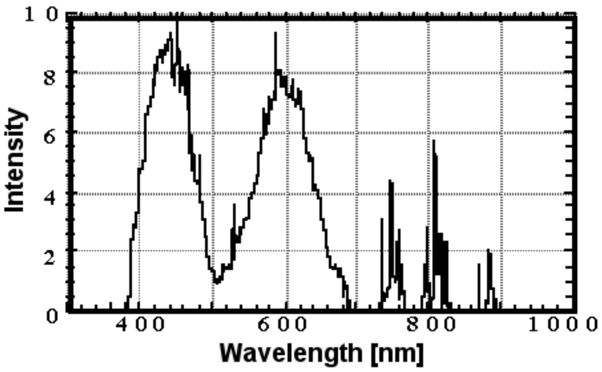

Fig. 8. Excitation spectrum of Cr and Nd codoped YAG at 1.06 μm.

difficult to dope into a single crystal, and of making new host ceramics having higher melting temperatures, such as Y_2O_3 and Zr2O_3.

2. Codoping Technology

Codoping of sensitizing ions is also available for YAG ceramics. Chromium codoping to Nd:YAG ceramics is effective for increasing the pumping efficiency by energy transfer from Cr to Nd [23]. In single crystal fabrication, the doping of Nd is limited to less than 1 %, and that of Cr to less than 0.1 % due to crystallization difficulty. However, the ceramic production process allows fabrication of 10-μm-sized crystals so that no limitation of doping appears up to 10 %. In codoping with Cr and Nd in YAG, the Cr ion is located at one of two types of aluminum-ion sites, and the Nd is arranged at the Yttrium-ion site.

Absorption of Cr;Nd:YAG is a summation of the absorptions of Cr and Nd ions. The excitation spectrum measured at the Nd emission of 1.06 μm in Fig. 8 shows an efficient energy transfer from Cr to Nd. Two broadband absorptions of the Cr^{3+} ion, one at 440 nm and the

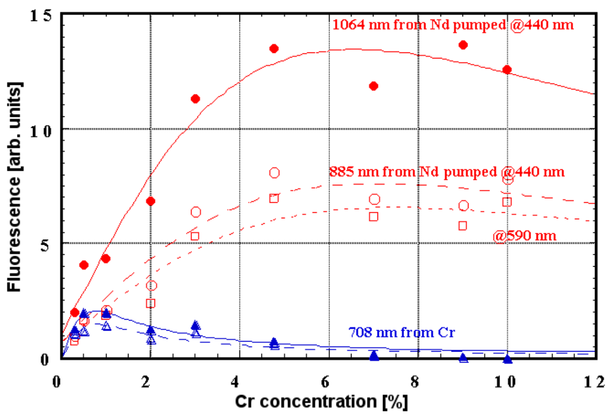

Fig. 9. Enhancement factor of fluorescence of Nd at 1.064 μm pumped at 440 nm and 590 nm of Cr and Nd codoped YAG.

other at 590 nm, may originate from transitions from the ^{4}A level to the T^1 and the T^2 levels.

The enhancement of the fluorescence of Nd at 1.064 μm pumped by the 440-nm and the 590-nm bands is shown in Fig. 9 as a function of the Cr^{3+} ion concentration. As the Cr concentration is increased, the fluorescence increases and reaches a maximum that is 13 times larger at a 6.5 % doping. In that figure, the fluorescence intensities of Nd at 885 nm and Cr at 708 nm are shown simultaneously. The fluorescence at 885 nm has similar concentration dependence as the 1.064-μm light, but the 708-nm fluorescence from the Cr ion has different characteristics. It is peaked at doping of 0.7 % and gradually decreases as the Cr concentration is increased. In a case of only Cr-doped YAG, the fluorescence at 708 nm had a maximum at about a 3 ∼ 4 % doping. This means that radiative coupling of the Cr ion to the Nd ion in YAG ceramics is very effective even if a concentration quenching of Cr ions occurs.

The lifetime of a spontaneous emission from the $^4F_{3/2}$ level of the Nd ion increases drastically by Cr codoping, as shown in Fig. 10 when Cr ions were pumped by 440-nm or 590-nm light. The energy transfer to Nd from

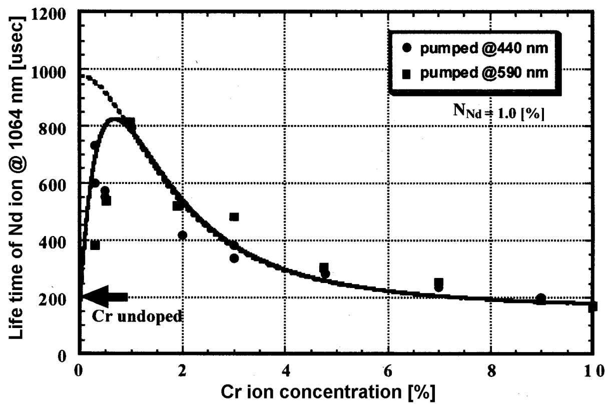

Fig. 10. Lifetime of 1.06-μm fluorescence of Nd:YAG is lengthened by Cr codoping.

Cr, with a long lifetime of 1.8 ms, sustains effectively a spontaneous energy decay of Nd. Maximum effective lifetime of the 1.06-μm emission reached 800 μs at a Cr concentration of 0.7 mol% in comparison with 210 μs in the case without Cr codoping.

In conclusion, ceramic materials such as YAG are very promising as average power laser materials with the potential for various doping with various laser atoms and sensitizing ions. The physics and engineering to grow materials should be developed to obtain more scatter-free grains and to optimize codoping with multiple ions in ceramics. Especially, the issues are the polarization characteristics, extending the growth possibility to various crystals, and precise measurement of the thermal and the mechanical properties as functions of the doping.

Ceramic materials have vast design potential due to the ensemble properties of small crystals. New material designs will be realized in near future, such as an emission-spectrum control, emission/absorption mixing materials, a layered composite structure, and a functional nano-sized structure, so on.

V. SUMMARY

This report describes recent topics in solid-state laser technologies related to peak-power- and high-energy-delivering systems. The OPCPA scheme is very promising for generation of a petawatt pulse with a large KDP crystal and a powerful pumping laser. A low prepulse level before a peak-power ultra-short pulse is important for laser-matter interaction experiments.

Phase conjugation technology can compensate for any thermal degradation in an average-power system, including a harmonic generation. Some problems are inherent in broadband operation of an SBS-PCM with a multimode laser beam, but a high laser-damage threshold is also expected in such system. Over a kilowatt of energy can be handled by a liquid-phase PCM with a flowing system or beam-moving optics.

Higher-energy delivery from a future laser system needs scalable materials for a solid-state laser. Transparent ceramics are good candidates, but more development, including co-doping fabrication, and more sophisticated material systems, such as emission-spectrum control materials, a combination of emission and absorption materials, layered composite structures, and functional nano-sized structures, is needed for potential optical devices.

ACKNOWLEDGMENTS

The authors thank Dr. T. Hatae and Mr. S. Kitamura for collaborative work on YAG laser development using an SBS-PCM at JAERI, Japan. We express our appreciation to Dr. T. Yanagitani, Kohnoshima Chemical Co. Ltd., Japan, and Prof. K. Ueda, Universityof Electro-communication, Japan, for their fruitful discussion on the ceramic material. This work was supported partially by a contract, No. 14350009, from the MEXT, Japanese government.

REFERENCES

[1] A. Dubeitis G. Jonusauskas and A. Piskarskas, Opt. Commun. **88**, 437 (1992).
[2] I. N. Ross P. Matousek, M. Towrie, A. J. Langley and J. L. Collier, Opt. Commun. **144**, 125 (1997).
[3] S. K. Zhang, M. Fujita, H. Yoshida, R. Kodama, H. Fujita, M. Nakatsuka, Y. Izawa and C. Yamanaka, SPIE **3886**, 588 (1999).
[4] H. Yoshida, E. Ishii, K. Sawai, R. Kodama, H. Fujita, Y. Kitagawa, S. Sakabe, Y. Izawa, T. Yamanaka and M. Fujita, CLEO '01 Tech. Digest **CMT7**, 99 (2001).
[5] H. Yoshida, E. Ishii, K. Sawai, R. Kodama, H. Fujita, Y. Kitagawa, S. Sakabe, Y. Izawa, T. Yamanaka and M. Fujita, CLEO/ PR '01 Tech. Digest **I-80** (2001).
[6] D. A. Rockwell, IEEE J. Quant. Electron. **24**, 1124 (1988).
[7] D. S. Sumida, D. C. Jones and D. A. Rockwell, IEEE J. Quant. Electron. **30**, 2617 (1994).
[8] C. B. Dane, L. E. Zapata, W. A. Neuman, M. A. Norton and L. A. Hackel, IEEE J. Quant. Electron. **31**, 148 (1995).
[9] H. L. Offerhaus, H. P. Godfried and W. J. Witteman, Opt. Commun. **128**, 61 (1996).
[10] R. J. Pierre, G. W. Holleman, M. Valley, H. Injeyan, J. G. Berg, G. M. Harpole, R. C. Hilyard, M. Mitchell, M. E. Weber, J. Zamel, T. Engler, D. Hall, R. Tinti and J. Machan, IEEE, J. Quant. Electron. **3**, 63 (1997).
[11] M. Bowers and R. W. Boyd, IEEE J. Quant. Electron. **34**, 634 (1998).
[12] G. A. Pasmanik, A. I. Makarov and A. A. Shilov, Laser and Particle Beams. **9**, 329 (1991).
[13] H. Yoshida,V. Kmetik, H. Fujita, M. Nakatsuka, T. Yamanaka and K. Yoshida, Appl. Opt. **36**, 3739 (1997).

[14] H. Yoshida, H. Fujita,M. Nakatsuka and K. Yoshida, Jpn. J. Appl. Phys. **38**, L521 (1999).
[15] T. Hatae, O. Nato, S. Kitamura, T. Sakuma, T. Hamano, Y. Tsukahara, M. Nakatsuka and H. Yoshida, Rev. Sci. Instruments **70**, 772 (1999).
[16] N. F. Andreev, E. Khazanov and G. E. Pasmanik, IEEE J. Quant. Electron. **28**, 330 (1992).
[17] H. Yoshida, H. Fujita, K. Yoshida and T. Yamanaka, Jpn. J. Optics **26**, 31 (1997) (in Japanese).
[18] H. Yoshida, A. Ohkubo, H. Fujitah and M. Nakatsuka, Rev. Laser Eng. **29**, 109 (2001) (in Japanese).
[19] M. Sekita, H. Haneda, T. Yanagitani and S. Shirasaki, J. Appl. Phys. **67**, 453 (1990).
[20] A. Ikesue, T. Kinoshita, K. Kamata and K. Yoshida, J. American Ceram. Soc. **78**, 1033 (1995).
[21] J. Lu, M. Prabhu, J. Xu, K. Ueda, H. Yagi, T. Yanagitani, A. Kaminskii, Jap. J. Appl. Phys. **39**, L1048 (2000).
[22] T. Yanagitani, private communication, Kohnoshima Chemical, Co. Ltd., Japan.
[23] M. Nakatsuka, H. Yoshida, Y. Fujimoto, K. Fujioka and H. Fujita, *Asian Pacific Laser Symposium 2002* (Osaka, Sep., 2002).